Articles in PresS. J Neurophysiol (February 2, 2011). doi:10.1152/jn.00537.2010

Muscle short-range stiffness can be used to estimate the endpoint stiffness of the human arm

Xiao Hu[1,2], Wendy M. Murray[1,2,3,4], Eric J. Perreault[1,2,3]

[1]Dept. of Biomedical Engineering, Northwestern University, Evanston, IL, USA
[2]Sensory Motor Performance Program, Rehabilitation Institute of Chicago, Chicago, IL, USA
[3]Dept. of Physical Medicine and Rehabilitation, Northwestern University, Chicago, IL, USA
[4]Research Service, Edward Hines, Jr. VA Hospital, Hines, IL, USA

Running title: Modeling endpoint stiffness of the human arm

Corresponding Author:
Eric J. Perreault
Department of Biomedical Engineering
Department of Physical Medicine and Rehabilitation
Northwestern University
345. E. Superior St.
Chicago, IL, USA 60611
e-perreault@northwestern.edu
1.312.238.2226
1.312.238.2208 (fax)

Abstract

The mechanical properties of the human arm are regulated to maintain stability across many tasks. The static mechanics of the arm can be characterized by estimates of endpoint stiffness, considered especially relevant for the maintenance of posture. At a fixed posture, endpoint stiffness can be regulated by changes in muscle activation, but which activation-dependent muscle properties contribute to this global measure of limb mechanics remains unclear. We evaluated the role of muscle properties in the regulation of endpoint stiffness by incorporating scalable models of muscle stiffness into a three-dimensional musculoskeletal model of the human arm. Two classes of muscle models were tested: one characterizing short-range stiffness, and two estimating stiffness from the slope of the force-length curve. All models were compared to previously collected experimental data describing how endpoint stiffness varies with changes in voluntary force. Importantly, muscle properties were not fit to the experimental data, but scaled only by the geometry of individual muscles in the model. We found that force-dependent variations in endpoint stiffness were accurately described by the short-range stiffness of active arm muscles. Over the wide range of evaluated arm postures and voluntary forces, the musculoskeletal model incorporating short-range stiffness accounted for 98±2%, 91±4% and 82±12% of the variance in stiffness orientation, shape and area, respectively, across all simulated subjects. In contrast, estimates based on muscle force-length curves were less accurate in all measures, especially stiffness area. These results suggest that muscle short-range stiffness is a major contributor to endpoint stiffness of the human arm. Furthermore, the developed model provides an important tool for assessing how the nervous system may regulate endpoint stiffness via changes in muscle activation.

Key words: Muscle short-range stiffness, Endpoint stiffness, Musculoskeletal model

54

55

Introduction

We commonly use our hands to move and manipulate objects in different environments. Many of these tasks tend to destabilize arm posture (Rancourt and Hogan 2001). Nevertheless, they can be completed because the central nerve system (CNS) regulates the mechanical properties of the arm to compensate for these instabilities, usually ensuring that the coupled system of the arm and its environment remains stable so that posture can be maintained (McIntyre et al. 1996). Understanding how this regulation occurs and the relative contributions of the nervous system and the intrinsic biomechanics of the arm remains an important problem in motor control.

Arm mechanics are typically quantified by applying controlled displacements, measuring the corresponding forces, and characterizing the relation between the two using estimates of arm impedance. The static component of impedance, known as stiffness, is thought to be especially important during the maintenance of posture. Estimates of endpoint stiffness are often used to summarize the mechanical properties of the whole arm at the endpoint, or point of contact with the environment (Mussa-Ivaldi et al. 1985). Many physiological mechanisms contribute to the forces measured in these experiments and to the corresponding estimates of endpoint stiffness. Actively controlled mechanisms at a specific arm posture include the intrinsic properties of the muscles within the arm, which are dependent on their steady state or feedforward activation, and transient changes in muscle activation that may occur via feedback pathways such as stretch reflexes or voluntary responses to the imposed displacements. While numerous studies have characterized the behavioral characteristics of endpoint stiffness (Burdet et al. 2001; Darainy et al. 2004; Franklin et al. 2003; Franklin et al. 2007; Gomi and Osu 1998; Perreault et al. 2001; Tsuji et al. 1995), and the feedback responses that may modulate this stiffness (Krutky et al. 2010; Perreault et al. 2008), few

have directly assessed which muscle properties contribute most to the stiffness properties of an entire limb. This knowledge is essential for understanding how changes in neural activation alter limb stiffness or how impairments to muscular or neuromotor systems may impact the ability to regulate stiffness in a contextually appropriate manner.

The intrinsic stiffness of individual muscles is undoubtedly a major contributor to the endpoint stiffness of the human arm. However, there has been little consensus regarding how muscle stiffness should be defined with respect to its contributions to the stiffness of an intact limb. A common approach has been to consider the slope of the force-length curve as the only activation-dependent stiffness component of muscle (Brown and Loeb 2000; Iqbal and Roy 2004; Stroeve 1999; Verdaasdonk et al. 2004). The slope of this curve may be scaled uniformly with changes in muscle activation or non-uniformly to represent the increasing length at which peak forces are generated for submaximal contractions (Rack and Westbury 1969). While the force-length curve describes the isometric force generated when a muscle is activated at different lengths, it does not describe how muscle force changes when length is changed (Joyce et al. 1969). For small rapid perturbations, the initial forces generated by a muscle can be described in terms of its short-range stiffness (Rack and Westbury 1974), which is thought to depend largely on the stiffness of the active cross-bridges acting in series with the passive structures of the muscle (Morgan 1977). It has been suggested that the short-range stiffness properties of muscle are a major factor in determining the stiffness of a joint (Bunderson et al. 2008; Colebatch and McCloskey 1987; Grillner 1972; Hufschmidt and Schwaller 1987; Joyce et al. 1974; Kirsch et al. 1994; Misiaszek 2006), but the importance of short-range stiffness has not been evaluated directly, particularly in the context of multijoint mechanics.

The primary objective of this work was to evaluate the hypothesis that the endpoint stiffness of the human arm can be accurately described by the intrinsic short-range stiffness of its active muscles, coupled to a realistic model of musculoskeletal geometry. This hypothesis was evaluated by adding scalable models of short-range stiffness (Cui et al. 2008) to an existing three-dimensional musculoskeletal model of the human upper limb (Holzbaur et al. 2005), and comparing the predictions of the resulting model to previously collected experimental data (Cannon and Zahalak 1982; Perreault et al. 2001). The efficacy of this model was compared to models that considered only the force-length properties of muscle. Our results clearly demonstrate that intrinsic muscle properties can account for previously reported variations in arm stiffness when short-range stiffness is considered, but not when using muscle models that consider only force-length properties. These results clarify how intrinsic muscle properties can contribute to the regulation of limb mechanics in the absence of neural feedback. Furthermore, experimental deviations from the model predictions can be used to identify situations in which neural control strategies beyond feedforward muscle activation are required to regulate arm stiffness in a task-appropriate manner. Portions of this work have been presented previously in abstract form (Hu et al. 2009a; Hu et al. 2009b).

Methods

Modeling

To evaluate the extent to which the endpoint stiffness produced during small, rapid perturbations is dominated by the short-range stiffness of active muscles, we performed simulations that coupled a musculoskeletal model of the upper limb with a scalable model of muscle stiffness. This muscle model estimates the short-range stiffness of a given muscle based on its geometry and active force (Cui et al. 2008). We compared these results with simulations that combined the same musculoskeletal model with muscle stiffness estimated using (i) the slope of the isometric force-length relationship during full activation (Zajac 1989), and (ii) the slope of the isometric force-length relationship, adjusted based on muscle activation level to reflect the shift in optimal fiber length with activation (Lloyd and Besier 2003).

The musculoskeletal model of the upper limb implemented in our study was adapted from the model described by Holzbaur *et al.* (2005). Our simulations incorporated kinematic representations of the shoulder and elbow joints, and included a total of 37 muscle segments. These segments corresponded to 9 shoulder muscles, separated into 15 segments; 14 elbow muscles, represented by 19 segments; and 2 biarticular muscles, represented by 3 segments. This model was used to obtain parameter values for optimal muscle fiber lengths, maximum isometric muscle forces, tendon slack lengths, and muscle moment arms, as needed for our simulations. Both the moment arms and the isometric force-generating capacity of the muscles estimated using this model vary as a function of joint posture. The parameter values in the musculoskeletal model describing the peak isometric forces for individual muscles were scaled from their original values (which were based on anatomical data collected in cadavers) using recent data describing both muscle volumes (Holzbaur et al. 2007b) and joint

148 strength (Holzbaur et al. 2007a) in the upper limb in the same healthy subjects. Similarly,
149 tendon slack length of the brachioradialis was decreased from the nominal value reported by
150 Holzbaur *et al*. (2005) to reflect recently reported intraoperative measurements (Murray et al.
151 2006). Finally, the flexion moment arm angle relationship of anterior deltoid was replaced by
152 the measurements reported by Kuechle *et al.* (1997), made in a posture more relevant to our
153 simulations; this change decreased the moment arm over the range of interest for this
154 manuscript.
155
156 Muscle short-range stiffness was estimated using the model developed by Cui et. al (2008),
157 for muscles in the cat hindlimb. The model assumes that the short-range stiffness of a
158 muscle-tendon unit, K, results from the stiffness of the muscle fibers, K^m, in series with the
159 stiffness of the tendon, K^t (Eq. 1).

$$K = \frac{K^m K^t}{(K^m + K^t)} \tag{1}$$

160 K^m is a function of muscle force (Eq. 2), F^m, optimal muscle fiber length at maximum
161 activation, l_0^m, and a dimensionless scaling constant $\gamma = 23.4$.

$$K^m = \frac{\gamma F^m}{l_0^m} \tag{2}$$

162
163 K^t was defined by the slope of the generic, dimensionless force-strain curve scaled for each
164 individual tendon (Zajac 1989). This is different than the scaling equation suggested by Cui
165 et al. (2008) since the geometric properties required for the Cui's tendon model were not
166 available for all of the muscles in our model. The impact of using a different tendon model
167 was assessed using the sensitivity analyses described below.
168

Estimation of muscle forces

Optimization was used to estimate the distribution of muscle forces for a specific set of joint torques. The cost function for this analysis was the sum of the squared muscle forces, expressed as a fraction of the maximum force for each muscle (Eq. 3) (Anderson and Pandy 2001; Crowninshield and Brand 1981). The problem was constrained such that 1) the resulting muscle forces summed to the specified joint torques (Eq. 4), and 2) muscle forces were positive and less than or equal to the maximum achievable forces at the current arm posture (Eq. 5). In these equations, F_i^m is the actual force and F_{i0}^m is the posture-dependent maximum isometric force for *i*th muscle respectively, r_{ij} is the posture-dependent moment arm for the *i*th muscle relative to the *j*th joint, and TQ_j is the torque about the *j*th joint. The summation over 37 elements corresponds to the number of muscle segments crossing the elbow and shoulder in our musculoskeletal model. The same cost function has been shown to work well in isometric force regulation tasks at arm postures similar to those used in the present study (Van Bolhuis and Gielen 1999).

$$u = \min \sum_{i=1}^{37} \left(\frac{F_i^m}{F_{i0}^m} \right)^2 \tag{3}$$

$$TQ_j = \sum_{i=1}^{37} r_{ij} \times F_i^m \quad i = 1,...,37; j = 1,2 \tag{4}$$

$$0 \le F_i^m \le F_{i0}^m \tag{5}$$

Model-based estimation of arm stiffness

Once muscle forces were estimated, we computed the corresponding joint and endpoint stiffnesses. The estimated force for each muscle (F_i^m) was used to calculate the corresponding short-range stiffness of the muscle-tendon unit, K_i, using Eqs. 1 and 2. Joint

stiffness (K^j) was calculated from muscle-tendon stiffness by considering the kinematic relationship between changes in joint angles and changes in muscle-tendon length (Eq. 6) (McIntyre et al. 1996).

$$K^j = J^T \vec{K} J + \frac{\partial J^T}{\partial \theta} \vec{F}^m \tag{6}$$

where θ is a vector describing the joint angles, J is the Jacobian matrix relating changes in muscle joint angles to changes in muscle length (it contains the moment arms of the muscles about the shoulder and elbow joints at the specified posture), $\vec{K}$ is a diagonal matrix in which the non-zero elements represent the stiffness for each muscle in the model, and $\vec{F}^m$ is the vector of muscle forces. The second term in the equation accounts for how angle dependent changes in muscle moment arms influence joint stiffness.

As described previously (McIntyre et al. 1996), endpoint stiffness (K^e) was computed from joint stiffness by considering the Jacobian (G) relating changes in joint angles to changes in endpoint displacement (Eq. 7).

$$K^e = \left(G^{-1}\right)^T \left[K^j - \frac{\partial G^T}{\partial \theta} F^{end} \right] G^{-1} \tag{7}$$

where F^{end} is the vector of endpoint forces.

Simulated experiments

The proposed model was used to simulate the endpoint stiffness measurements made in a previously published study (Perreault et al. 2001). Endpoint stiffness can be visualized as an

ellipse (Mussa-Ivaldi et al. 1985). Such representations typically are quantified by area (a measure of magnitude), orientation (the direction of maximal endpoint stiffness), and shape (a measure of stiffness anisotropy). These parameters were computed as described previously (Gomi and Osu 1998) and used to compare the model-based estimates of endpoint stiffness to those measured experimentally.

The experimental measurements involved estimating endpoint stiffness as subjects exerted constant levels of endpoint force against a rigid manipulator. All measurements were made in the horizontal plane with a shoulder abduction angle of 90° and are described in detail in the original publication (Perreault et al. 2001). In summary, the subjects' hands were positioned either directly in front of the sternum (medial posture), in front of the shoulder (central posture), or lateral to the shoulder (lateral posture). For the purpose of our endpoint stiffness simulations, we selected data corresponding to all five subjects tested in the previous study. We simulated the endpoint stiffness of these subjects at four endpoint force magnitudes, corresponding to 7.5%, 15%, 22.5%, and 30% of the subjects' maximum voluntary contractions. These forces were oriented along one of four directions ($\pm X$, lateral and medial; and $\pm Y$, anterior and posterior). Using the model, joint torques (TQ) were calculated from the measured endpoint forces (F^{end}) using the standard relation shown in Eq.8.

$$TQ = G^T F^{end} \tag{8}$$

Given these joint torques, a model-based estimate of endpoint stiffness could be obtained by solving Equations 1-7, as described above. Experimental estimates made under passive conditions were used to define the passive properties of the joints within the model.

We also compared model-based estimates of elbow stiffness to those obtained from the

multi-joint experimental study described above and to those measured in a previously published single-joint experiment (Cannon and Zahalak 1982). For these estimates, the model was compared to the previously published group results to obtain estimates of the expected experimental variability across subjects. All predictions were restricted to elbow moments between -20 to 20 Nm, to remain within the range of previously reported experimental results.

Model comparisons

As an alternative to characterizing muscle stiffness, K^m, by estimates of short-range stiffness, we also estimated muscle stiffness as the slope of the force-length relationship, and then used Eq. 1 to compute the total stiffness of the muscle-tendon unit. Tendon stiffness was kept the same for both methods. The force-length relationship implemented in SIMM (Delp and Loan 2000) was used for muscle stiffness estimation. It uses a force-length relationship defined by a dimensionless curve (Delp and Loan 2000; Zajac 1989). The slope of the curve, scaled by the muscle activation level, was defined as the muscle fiber stiffness. The activation level for a given muscle was specified by the force in the muscle that resulted from the optimization, normalized by the maximum isometric force the muscle could produce at the arm posture of interest, as defined by the musculoskeletal model.

It is well known that the peak of the force-length curve for a muscle shifts to longer muscle lengths at submaximal levels of activation (Rack and Westbury 1969; Roszek et al. 1994). To take this characteristic into account, the following relationship developed by Lloyd and Besier (2003) was also evaluated in this study:

$$l_0^m(t) = l_0^m\left[\lambda\left(1-a(t)\right)+1\right] \qquad (9)$$

where λ is the percentage change in optimal fiber length, $a(t)$ the activation at time t, $l_0^m(t)$

256 the optimal fiber length at time t and activation $a(t)$. λ was chosen as 0.15, which means the
257 optimal fiber length is 15% longer at zero activation (Lloyd and Besier 2003).
258
259 The activation $a(t)$ in Eq. 9 was determined in a different way from that used for
260 activation-independent force-length curve. First, for each muscle, the force resulting from the
261 optimization was used in a force balance equation to calculate the force in the tendon and,
262 therefore, the tendon length. Next, muscle fiber length was determined by subtracting the
263 calculated tendon length from the musculotendon length, which was explicitly defined by the
264 musculoskeletal model as a function of arm geometry. The combination of muscle force and
265 fiber length that resulted from this process uniquely determined activation.
266
267 *Sensitivity analysis*
268 Due to the unavoidable variability in physiologic parameters, Monte Carlo analyses (Hughes
269 and An 1997; Santos and Valero-Cuevas 2006) were conducted to evaluate the sensitivity of
270 our model-based estimates of endpoint stiffness to four types of model parameters: muscle
271 moment arms, tendon stiffness, joint angles, and the maximum isometric force of each
272 muscle. This analysis was done at the maximum endpoint forces measured in the
273 experimental study (30% MVC) along each of the four voluntary force directions ($\pm X$ and
274 $\pm Y$). For each set of simulations, model parameters were selected from a normal distribution
275 centered about the nominal parameter values defined by our model with a standard deviation
276 that was equal to the plausible range over which these parameters could be expected to vary
277 across different individuals, as defined by experimental data reported in the literature.
278 Standard deviations for tendon stiffnesses and muscle moment arms were set to 25% and
279 20% of the nominal parameter values, respectively (Murray et al. 2002; Zajac 1989).
280 Standard deviations for joint angles were set to 4 degrees, the accuracy with which joint

281 posture can be measured with a goniometer (Fish and Wingate 1985; Grohmann 1983).
282
283 The plausible range of peak muscle forces was estimated by typical variations in muscle
284 volume. The maximum force a muscle can produce is determined by its physiological
285 cross-sectional area (PCSA). PCSA is a measure of the muscle's total volume, normalized by
286 fiber length and adjusted by pennation angle so that the maximum isometric force-generating
287 capability of muscles with different lengths and orientations of fibers can be compared
288 directly, based only on anatomical measurements (Spector et al. 1980). When comparing the
289 same muscle (i.e., the triceps brachii from a small female to the triceps brachii of a large
290 male), differences in muscle volume dominate inter-subject variability. For example, the
291 relative variance (standard deviation/mean) of triceps volume was 47% in a study of 10
292 healthy subjects spanning a large size range (Holzbaur et al. 2007b). In contrast, optimal
293 fascicle length in triceps long head varied by only 17% in a cadaver study that included a
294 comparable range of specimen sizes (Murray et al. 2000). Total muscle volume in the upper
295 limb varied threefold across young healthy subjects, while volume fraction (defined as
296 individual muscle volume/total muscle volume) had a standard deviation of approximately
297 20 percent on average (Holzbaur et al. 2007b). Variation in volume fraction was used to
298 assess the sensitivity of our stiffness estimates to the uncertainty in our parameters defining
299 relative muscle strength within a given subject. Changes in absolute strength across subjects
300 were assessed separately, as described below.
301
302 The influence of variability in moment arms, tendon stiffness, joint angles, and muscle
303 volume fraction on our results was assessed independently. Three hundred simulations were
304 performed per set, for a total of 1,200 simulations (4 parameter types x 300 individual
305 simulations). In each individual simulation, the parameter of interest was selected randomly

306 for each muscle (or joint for simulations that explored variability in joint posture).
307
308 The results of these simulations were summarized by the standard deviation of the endpoint
309 stiffness characteristics described previously: area, orientation and shape. The sensitivity of
310 each model output to a given parameter was reported as the standard deviation of the output
311 across the 300 Monte Carlo simulations performed for each parameter. The standard
312 deviations of estimated stiffness area and shape were normalized by their nominal values.
313 The standard deviation of the estimated endpoint stiffness orientation, however, was
314 described in absolute units since the nominal values depend on the defined coordinate system
315 orientation and are not meaningful for these purposes.
316
317 The isometric strength of our model is based on average data describing young, healthy male
318 subjects (Holzbaur et al. 2007a). To examine the influence of variations in absolute strength
319 on our results, we scaled the muscle volumes in the nominal model (total muscle volume =
320 3600.6 cm^3) to reflect 3 sets of subject-specific data reported in the literature (Holzbaur et al.
321 2007b). (smallest female subject, total muscle volume = 1426.9 cm^3; smallest male subject,
322 total muscle volume = 2954.8 cm^3; and largest male subject, total muscle volume = 4426.8
323 cm^3). These results are reported independently from the Monte Carlo analyses.
324

Results

Model-based estimation of elbow stiffness

The developed model characterized many important features of how elbow stiffness varied with changes in elbow torque. The simulated elbow stiffness increased with increasing elbow torque and was larger in flexion than in extension, as has been documented experimentally (Figure 1). For all simulated subjects, the predictions of how elbow stiffness varied with changes in elbow flexion torque fell within the 95% confidence intervals for the average data reported in two experimental studies (Cannon and Zahalak 1982; Perreault et al. 2001). The model-based estimates of elbow stiffness during flexion were at most 13±2% and 21±3% higher than the average experimental results reported by Cannon and Perreault, respectively. Larger differences were found for the predictions of how elbow stiffness varied with changes in elbow extension torque. For extension, the model-based estimates were lower than the experimental results reported by Cannon and Perreault by up to 21±1% and 30±1%, respectively.

Model-based estimation of endpoint stiffness

The model-based estimates of endpoint stiffness were similar to the experimental results in orientation, shape and area over the full range of tested forces and postures across all subjects. Typical model estimates for a single subject (No.4) is shown in Figure 2. On average, the model accounted for 98±2% of the variation in stiffness orientation across all tested conditions. Over the same range of conditions, the model accounted for an average of 91±4% and 82±12% of the variability in stiffness shape and area, respectively (Table 1).

Stiffness estimation from the force-length relationship

Model-based stiffness estimates based on the slope of the force-length curve dramatically

underestimated the magnitude of joint and endpoint stiffness. For elbow joint stiffness, estimations from the force-length relationship were much lower than the 95% confidence intervals reported in both experimental studies (Cannon and Zahalak 1982; Perreault et al. 2001) (Figure 3A, typical data of subject No. 4). The simulated elbow stiffness was up to 82±3% and 82±1% lower than the experimental stiffness for both flexion and extension. Small improvements were observed when using the modified force-length relationship (Lloyd and Besier 2003). These improvements were largely for elbow flexion, although these model-based estimates were still lower than the experimental estimates by more than 69±8%. No substantial improvements were observed for elbow extension, in which the model-based estimates remained more than 79±2% lower than the experimental estimates.

The model-based estimates of endpoint stiffness obtained using the slope of the force-length curve also were much smaller than the experimental estimates (Figure 3B, typical data of subject No. 4). Specifically, the estimation only accounted for 13±2% of variance in the area of stiffness ellipses at the central arm position, though it accounted for 84±7% and 57±22% of variance in the orientation and shape at the same arm position (Table 1). Applying the coupled force-length relationship gave similar results, accounting for only 20±6% of variance in the area. The area of ellipses represents the magnitude of endpoint stiffness, thus the estimation from both types of force-length relationships greatly underestimated the magnitude of the measured endpoint stiffness.

Sensitivity analysis

The model-based estimates of endpoint stiffness were relatively insensitive to changes of model parameters. The maximum expected errors in the estimated endpoint stiffness orientation, shape and area were 6.3 degrees, 22% and 23%, respectively (Table 2).

Model-based estimates of endpoint stiffness generally were most sensitive to errors in model moment arms, volume fraction and joint angles. The model-based estimates were approximately an order of magnitude less sensitive to errors in the estimated tendon properties. Orientation was most sensitive to changes in joint angles, although even this sensitivity was small, resulting in a maximum expected orientation error of less than 7 degrees. Endpoint stiffness shape and area were most sensitive to uncertainty in moment arm values. Again, these sensitivities were small, resulting in expected errors less than 25% for parameter errors at the maximum of the plausible range.

Changes in total muscle volume also did not substantially influence the model predictions. From smallest (M1) to the largest (M5) male subjects (total muscle volume increased by 50%), the variation in the model output relative to the nominal parameter values was lower than 2 deg for the orientation (Figure 4A) and 10% for the shape and the area (Figure 4B). For the smallest female (F1), the variation in the model output was about 4 deg for endpoint stiffness orientation (Figure 4A) and 15% for the shape and the area (Figure 4B). Though the model worked best with male subjects, which the nominal parameter values represented, it also gave reasonably good estimates for the smallest female subject (~4 deg variation in the orientation and ~15% variation in the shape and the area), whose total muscle volume was approximately only 40% of the average male subject represented by our model.

Discussion

The purpose of this study was to quantify the degree to which the endpoint stiffness of the human arm could be attributed to the short-range stiffness of the active muscles within the arm. This was accomplished by combining scalable models of short-range stiffness with a 3D musculoskeletal model of the upper limb and evaluating how well this combined model could explain previously collected experimental data. We found that the combined model accurately described the variation in endpoint stiffness across a range of arm postures and voluntary forces. Importantly, these predictions were made without fitting any model parameters to the experimental data. In contrast, muscle stiffness estimates obtained from the slope of the force-length curve were unable to describe the experimentally measured variations in endpoint stiffness. These results suggest that the short-range stiffness of muscles within the arm is a major contributor to endpoint stiffness. Furthermore, the model we have developed provides an important tool for assessing how the nervous system can regulate endpoint stiffness via changes in muscle co-contraction in addition the reciprocal activation needed to generate the forces for a specific task.

Muscle properties contributing to endpoint stiffness

Our results suggest that short-range stiffness is a major contributor to the endpoint stiffness of the human arm. It is important, however, to consider the experimental conditions used to estimate endpoint stiffness. Isolated muscles exhibit short-range stiffness when stretched less than 2-3% of the muscle fiber length or through movements covering approximately 3-4% of the physiological range (Rack and Westbury 1974). The perturbations used in the experiments we considered (Perreault et al. 2001) did not exceed this range. Those perturbations had peak-to-peak amplitudes of 2 cm, which generated maximum movements of approximately 3 degrees at the shoulder and 2 degrees at the elbow. These joint rotations

represent approximately only 2% of the range of motion for these joints within the horizontal plane, well within the limits of short-range stiffness. It is likely that experiments incorporating larger perturbations would not be so well characterized by our current model. Indeed, it has been demonstrated that the estimated stiffness of single and multijoint systems decreases with increasing perturbation amplitude (Kearney and Hunter 1982; Shadmehr et al. 1993), as would be expected when muscle exceed their region of short-range stiffness (Rack and Westbury 1974). Beyond this range, more complex models that consider the dynamics of cross-bridge cycling would likely be necessary.

Endpoint stiffness cannot be described by the slope of the force-length curve, even though this has commonly been assumed to approximate the stiffness properties of individual muscles. The force-length curve represents the isometric force that a muscle can generate at a specific length, rather than the change in muscle force that occurs with rapid changes in length, as are required to estimate stiffness. These two properties are known to differ (Joyce et al. 1969). The force-length properties are determined largely by the overlap of the actin and myosin filaments at different muscle lengths (Gordon et al. 1966), whereas the short-range stiffness properties are thought to arise from the number of bound cross-bridges (Morgan 1977; Rack and Westbury 1974). In contrast to the slope of the force-length curve, short-range stiffness is length-independent and changes primarily with changes in muscle force (Morgan 1977), which greatly simplifies the problem of estimating muscle contributions to limb mechanics at different postures.

It is important to note that stiffness is only one component of muscle and limb impedance. Inertial, viscous and higher order properties also contribute substantially to the mechanical properties of a limb. Our model focuses only on limb stiffness, which has been proposed to

play an important role in the control of posture and movement (Hogan 1985), and to contribute to limb stability during different tasks that destabilize limb posture (Burdet et al. 2001; Selen et al. 2009). We have demonstrated how muscle short-range stiffness contributes to the limb stiffness of the entire limb. Identifying a similar relationship for limb viscosity would allow for a more complete description of how intrinsic muscle properties contribute to the mechanical properties of a limb in the absence of changes in muscle activation resulting from neural control.

Influence of muscle activation on estimates of endpoint stiffness

Short-range stiffness scales with muscle force and the accuracy of our endpoint stiffness model depends upon the accuracy with which individual muscle forces can be estimated. Due to the redundant nature of the musculoskeletal system, we used optimization to estimate the individual muscle forces contributing to the endpoint forces measured during the experimental studies. We selected a common cost function that minimizes the relative activation of all muscles (Anderson and Pandy 2001; Crowninshield and Brand 1981) and which has been shown to work well during isometric the force regulation tasks (Van Bolhuis and Gielen 1999) relevant to our study. Such a cost function, however, does not predict co-contraction of antagonistic muscles (Collins 1995), and is certain to be inadequate in tasks that require co-contraction, thereby altering limb stiffness without corresponding changes in net joint torque (Gomi and Osu 1998; Milner et al. 1995). These limitations may have contributed to the low values of elbow stiffness predicted by our model during extension tasks. Nevertheless, the majority of our predictions were surprisingly accurate given that our model was not fit to the experimental data. This is likely due to the presence of minimal co-contraction in the experiments we attempted to replicate in simulation. For tasks with substantial co-contraction, different methods will be needed for estimating individual muscle

forces, such as EMG assisted optimization (Cholewicki and McGill 1994).

Sensitivity of model predictions to parameter errors

Our predictions of endpoint stiffness were robust with respect to changes in model parameters that were within the range of plausible variations. Endpoint stiffness predictions were most sensitive to changes in model geometry, such as moment arms and joint angles, emphasizing the need to use realistic musculoskeletal models when assessing the contributions of muscle properties to endpoint stiffness. Our model was not sensitive to changes in total muscle volume and was moderately sensitive to the volume fraction of individual muscles. The latter sensitivity is likely due to the optimization algorithm used to estimate muscle forces. Crowninshield and Brand (1981) noted that the optimization algorithm we employed tended to allocate more force to stronger muscles. This redistribution would alter the relative contributions of synergistic muscles to the net joint torques and also stiffness. This redistribution of synergistic forces would affect limb stiffness only for muscles with different geometric properties, such as fiber lengths (Eq. 2) or moment arms (Eq. 6).

Model predictions were least sensitive to changes in tendon stiffness. This is likely due to the fact that short-range stiffness is dominated by muscle stiffness at low activation levels (Cui et al. 2007), and that the maximum endpoint forces assessed in this study never exceeded 30% of the maximum strength. Tendon stiffness may play a more important role at higher force levels and for muscles with relatively long tendons, such as those in the distal parts of the upper and lower limbs. In those cases, our assumption of uniform material properties for all tendons, which is known to be incorrect (Bennett et al. 1986; Cui et al. 2009; Zajac 1989), may lead to larger prediction errors.

Feedback contributions to endpoint stiffness

Our model predicts how steady-state changes in muscle activation, such as those usually attributable to voluntary feedforward motor commands, contribute to changes in endpoint stiffness. The model does not explicitly represent contributions from feedback pathways. As a result, it may fail to characterize endpoint stiffness estimated using protocols in which transient feedback responses to an applied perturbation contribute substantially to the net endpoint force. The modeled experiments (Perreault et al. 2001) used continuous stochastic perturbations to estimate endpoint stiffness. The fact that our model accurately described the stiffness estimated in those experiments suggests either that feedback contributions were small, as has been reported previously for perturbations with a high average velocity (Kearney et al. 1997), or that the muscle contractions were largely fused. During fused contractions, feedback would largely serve to increase the tonic force level.

Feedback responses to transient perturbations of endpoint position can be large (Krutky et al. 2010; Perreault et al. 2008), and protocols that use transient perturbations to estimate endpoint stiffness (Burdet et al. 2001; Darainy et al. 2004; Franklin et al. 2007) may not be well represented by our model. Deviations between our model predictions and stiffness estimates made using transient perturbations may be useful for beginning to assess reflex contributions to the regulation of endpoint stiffness.

Comparison with other models of endpoint stiffness

Due to its importance in understanding how the nervous system regulates the mechanical properties of the arm, there have been numerous attempts to develop models of endpoint stiffness. While each has contributed to our understanding of stiffness regulation, we are unaware of any that have incorporated 3D musculoskeletal geometry or that have directly

assessed which muscle properties are most relevant to stiffness regulation. Many models have considered stiffness regulation only at the joint level (Flash and Mussa-Ivaldi 1990; Gomi and Osu 1998; Tee et al. 2004). Those models that have directly incorporated muscles (Osu and Gomi 1999; Shin et al. 2009; Tee et al. 2010), have considered only a reduced muscle set and constant moment arms, at times selected for computational simplicity or to best fit the experimental data. While these assumptions have been sufficient for the intended purposes, they may not readily allow for generalization to novel situations, especially given our finding that stiffness estimates are most sensitive to the geometric properties of the model.

Models also have been developed that incorporate more complex mechanisms, including muscle dynamics in the form of Hill-type models and feedback pathways to represent reflex behaviors (Gribble et al. 1998; Stroeve 1999). Neither model incorporated short-range stiffness. While both models have been shown to generalize across conditions, their complexity makes is difficult to assess which of the modeled mechanisms are most relevant to the simulated behaviors. Interestingly, Stroeve (1999) suggested that reflexes are a major contributor to the simulated endpoint stiffness, but noted that the Hill-type models used in his simulations do "not fully represent the intrinsic, low-frequency components of the impedance." Wagner & Blickhan (1999) reached similar conclusions, by evaluating how muscle properties contribute to postural stability during standing. They concluded that simple Hill-type models were not able to maintain stability. Stable postures could be obtained only with sufficiently large parallel stiffness, as could be provided by the short-range stiffness of active cross-bridges, or with sufficient feedback control. Our model provides a direct means to evaluate the contributions that can be expected from the intrinsic stiffness of muscle in the absence of feedback. Failure to incorporate these intrinsic properties of muscle

545 may lead to an overestimation of the role that feedback plays in the regulation of limb
546 mechanics and stability.
547
548 In contrast to previous models of endpoint stiffness, we have developed a mechanistically
549 simple model that is able to replicate measures of endpoint stiffness without explicitly fitting
550 any parameters to the experimental data. This was done by incorporating experimentally
551 validated, scalable models of muscle short-range stiffness into a realistic musculoskeletal
552 model of the human arm. This provides us with a means to assess how the nervous system
553 may regulate endpoint stiffness via changes in the steady-state activation of arm muscles.
554

555 # References

556 **Anderson FC, and Pandy MG**. Static and dynamic optimization solutions for gait are practically equivalent. *J*

557 *Biomech* 34: 153-161, 2001.

558 **Bennett M, Ker R, Dimery N, and Alexander R**. Mechanical properties of various mammalian tendons.

559 *Journal of zoology Series A* 209: 537-548, 1986.

560 **Brown I, and Loeb G**. A reductionist approach to creating and using neuromusculoskeletal models.

561 *Biomechanics and neural control of posture and movement* 148-163, 2000.

562 **Bunderson N, Burkholder T, and Ting L**. Reduction of neuromuscular redundancy for postural force

563 generation using an intrinsic stability criterion. *J Biomech* 41: 1537-1544, 2008.

564 **Burdet E, Osu R, Franklin DW, Milner TE, and Kawato M**. The central nervous system stabilizes unstable

565 dynamics by learning optimal impedance. *Nature* 414: 446-449, 2001.

566 **Cannon SC, and Zahalak GI**. The mechanical behavior of active human skeletal muscle in small oscillations.

567 *J Biomech* 15: 111-121, 1982.

568 **Cholewicki J, and McGill S**. EMG assisted optimization: a hybrid approach for estimating muscle forces in an

569 indeterminate biomechanical model. *J Biomech* 27: 1287-1289, 1994.

570 **Colebatch J, and McCloskey D**. Maintenance of constant arm position or force: reflex and volitional

571 components in man. *The Journal of Physiology* 386: 247-261, 1987.

572 **Collins J**. The redundant nature of locomotor optimization laws. *J Biomech* 28: 251-267, 1995.

573 **Crowninshield RD, and Brand RA**. A physiologically based criterion of muscle force prediction in

574 locomotion. *J Biomech* 14: 793-801, 1981.

575 **Cui L, Maas H, Perreault E, and Sandercock T**. In situ estimation of tendon material properties: Differences

576 between muscles of the feline hindlimb. *J Biomech* 42: 679-685, 2009.

577 **Cui L, Perreault EJ, Maas H, and Sandercock TG**. Modeling short-range stiffness of feline lower hindlimb

578 muscles. *J Biomech* 41: 1945-1952, 2008.

579 **Cui L, Perreault EJ, and Sandercock TG**. Motor unit composition has little effect on the short-range stiffness

580 of feline medial gastrocnemius muscle. *J Appl Physiol* 103: 796-802, 2007.

581 **Darainy M, Malfait N, Gribble PL, Towhidkhah F, and Ostry DJ**. Learning to control arm stiffness under

582 static conditions. *J Neurophysiol* 92: 3344-3350, 2004.

583 **Delp SL, and Loan JP**. A computational framework for simulating and analyzing human and animal

584 movement. *Computing in Science & Engineering* 2: 46-55, 2000.

585 **Fish DR, and Wingate L**. Sources of goniometric error at the elbow. *Phys Ther* 65: 1666-1670, 1985.

586 **Flash T, and Mussa-Ivaldi F**. Human arm stiffness characteristics during the maintenance of posture. *Exp*

587 *Brain Res* 82: 315-326, 1990.

588 **Franklin DW, Burdet E, Osu R, Kawato M, and Milner TE**. Functional significance of stiffness in

589 adaptation of multijoint arm movements to stable and unstable dynamics. *Exp Brain Res* 151: 145-157, 2003.

590 **Franklin DW, Liaw G, Milner TE, Osu R, Burdet E, and Kawato M**. Endpoint stiffness of the arm is

591 directionally tuned to instability in the environment. *J Neurosci* 27: 7705-7716, 2007.

592 **Gomi H, and Osu R**. Task-dependent viscoelasticity of human multijoint arm and its spatial characteristics for

interaction with environments. *J Neurosci* 18: 8965-8978, 1998.

Gordon A, Huxley A, and Julian F. The variation in isometric tension with sarcomere length in vertebrate muscle fibres. *The Journal of Physiology* 184: 170-192, 1966.

Gribble PL, Ostry DJ, Sanguineti V, and Laboissiere R. Are complex control signals required for human arm movement? *J Neurophysiol* 79: 1409-1424, 1998.

Grillner S. The role of muscle stiffness in meeting the changing postural and locomotor requirements for force development by the ankle extensors. *Acta Physiol Scand* 86: 92-108, 1972.

Grohmann JEL. Comparison of two methods of goniometry. *Phys Ther* 63: 922-925, 1983.

Hogan N. The mechanics of multi-joint posture and movement control. *Biol Cybern* 52: 315-331, 1985.

Holzbaur KRS, Delp SL, Gold GE, and Murray WM. Moment-generating capacity of upper limb muscles in healthy adults. *J Biomech* 40: 2442-2449, 2007a.

Holzbaur KRS, Murray WM, and Delp SL. A model of the upper extremity for simulating musculoskeletal surgery and analyzing neuromuscular control. *Ann Biomed Eng* 33: 829-840, 2005.

Holzbaur KRS, Murray WM, Gold GE, and Delp SL. Upper limb muscle volumes in adult subjects. *J Biomech* 40: 742-749, 2007b.

Hu X, Murray WM, and Perreault EJ. Modeling muscle contributions to multijoint mechanics. In: *2009 Annual Meeting of Society for Neuroscience*. Chicago, IL: 2009a.

Hu X, Murray WM, and Perreault EJ. Modeling muscle contributions to multijoint mechanics. In: *33th Annual Meeting of American Society Biomechanics*. State College, PA, USA: 2009b.

612 **Hufschmidt A, and Schwaller I**. Short-range elasticity and resting tension of relaxed human lower leg muscles.
613 *The Journal of Physiology* 391: 451-465, 1987.
614 **Hughes R, and An K**. Monte Carlo simulation of a planar shoulder model. *Med Biol Eng Comput* 35: 544-548,
615 1997.
616 **Iqbal K, and Roy A**. Stabilizing PID controllers for a single-link biomechanical model with position, velocity,
617 and force feedback. *J Biomech Eng* 126: 838-843, 2004.
618 **Joyce G, Rack P, and Ross H**. The forces generated at the human elbow joint in response to imposed sinusoidal
619 movements of the forearm. *The Journal of Physiology* 240: 351-374, 1974.
620 **Joyce GC, Rack PM, and Westbury DR**. The mechanical properties of cat soleus muscle during controlled
621 lengthening and shortening movements. *The Journal of Physiology* 204: 461-474, 1969.
622 **Kearney R, and Hunter I**. Dynamics of human ankle stiffness: variation with displacement amplitude. *J*
623 *Biomech* 15: 753-756, 1982.
624 **Kearney RE, Stein RB, and Parameswaran L**. Identification of intrinsic and reflex contributions to human
625 ankle stiffness dynamics. *IEEE Trans Biomed Eng* 44: 493-504, 1997.
626 **Kirsch RF, Boskov D, and Rymer WZ**. Muscle stiffness during transient and continuous movements of cat
627 muscle: perturbation characteristics and physiological relevance. *Biomedical Engineering, IEEE Transactions*
628 *on* 41: 758-770, 1994.
629 **Krutky MA, Ravichandran VJ, Trumbower RD, and Perreault EJ**. Interactions between limb and
630 environmental mechanics influence stretch reflex sensitivity in the human arm. *J Neurophysiol* 103: 429-440,

2010.

Kuechle DK, Newman SR, Itoi E, Morrey BF, and An K-N. Shoulder muscle moment arms during horizontal flexion and elevation. *J Shoulder Elbow Surg* 6: 429-439, 1997.

Lloyd DG, and Besier TF. An EMG-driven musculoskeletal model to estimate muscle forces and knee joint moments in vivo. *J Biomech* 36: 765-776, 2003.

McIntyre J, Mussa-Ivaldi FA, and Bizzi E. The control of stable postures in the multijoint arm. *Exp Brain Res* 110: 248-264, 1996.

Milner TE, Cloutier C, Leger AB, and Franklin DW. Inability to activate muscles maximally during cocontraction and the effect on joint stiffness. *Exp Brain Res* 107: 293-305, 1995.

Misiaszek J. Control of frontal plane motion of the hindlimbs in the unrestrained walking cat. *J Neurophysiol* 96: 1816, 2006.

Morgan DL. Separation of active and passive components of short-range stiffness of muscle. *Am J Physiol Cell Physiol* 232: C45-49, 1977.

Murray W, Hentz V, Friden J, and Lieber R. Variability in surgical technique for brachioradialis tendon transfer. Evidence and implications. *The Journal of Bone and Joint Surgery* 88: 2009, 2006.

Murray WM, Buchanan TS, and Delp SL. The isometric functional capacity of muscles that cross the elbow. *J Biomech* 33: 943-952, 2000.

Murray WM, Buchanan TS, and Delp SL. Scaling of peak moment arms of elbow muscles with upper extremity bone dimensions. *J Biomech* 35: 19-26, 2002.

Mussa-Ivaldi FA, Hogan N, and Bizzi E. Neural, mechanical, and geometric factors subserving arm posture in humans. *J Neurosci* 5: 2732-2743, 1985.

Osu R, and Gomi H. Multijoint muscle regulation mechanisms examined by measured human arm stiffness and EMG signals. *J Neurophysiol* 81: 1458-1468, 1999.

Perreault E, Kirsch R, and Crago P. Effects of voluntary force generation on the elastic components of endpoint stiffness. *Exp Brain Res* 141: 312-323, 2001.

Perreault EJ, Chen K, Trumbower RD, and Lewis G. Interactions with compliant loads alter stretch reflex gains but not intermuscular coordination. *J Neurophysiol* 99: 2101-2113, 2008.

Rack PM, and Westbury DR. The effects of length and stimulus rate on tension in the isometric cat soleus muscle. *The Journal of Physiology* 204: 443-460, 1969.

Rack PMH, and Westbury DR. The short range stiffness of active mammalian muscle and its effect on mechanical properties. *J Physiol* 240: 331-350, 1974.

Rancourt D, and Hogan N. Dynamics of pushing. *Journal of motor behavior* 33: 351-362, 2001.

Roszek B, Baan G, and Huijing P. Decreasing stimulation frequency-dependent length-force characteristics of rat muscle. *J Appl Physiol* 77: 2115-2124, 1994.

Santos V, and Valero-Cuevas F. Reported anatomical variability naturally leads to multimodal distributions of Denavit-Hartenberg parameters for the human thumb. *IEEE Trans Biomed Eng* 53: 155, 2006.

Selen L, Franklin D, and Wolpert D. Impedance Control Reduces Instability That Arises from Motor Noise. *J Neurosci* 29: 12606, 2009.

669 **Shadmehr R, Mussa-Ivaldi F, and Bizzi E**. Postural force fields of the human arm and their role in generating
670 multijoint movements. *J Neurosci* 13: 45-62, 1993.
671 **Shin D, Kim J, and Koike Y**. A myokinetic arm model for estimating joint torque and stiffness from EMG
672 signals during maintained posture. *J Neurophysiol* 101: 387-401, 2009.
673 **Spector SA, Gardiner PF, Zernicke RF, Roy RR, and Edgerton VR**. Muscle architecture and force-velocity
674 characteristics of cat soleus and medial gastrocnemius: implications for motor control. *J Neurophysiol* 44:
675 951-960, 1980.
676 **Stroeve S**. Impedance characteristics of a neuromusculoskeletal model of the human arm I. Posture control.
677 *Biol Cybern* 81: 475-494, 1999.
678 **Tee K, Franklin D, Kawato M, Milner T, and Burdet E**. Concurrent adaptation of force and impedance in the
679 redundant muscle system. *Biol Cybern* 102: 31-44, 2010.
680 **Tee KP, Burdet E, Chew CM, and Milner TE**. A model of force and impedance in human arm movements.
681 *Biol Cybern* 90: 368-375, 2004.
682 **Tsuji T, Morasso P, Goto K, and Ito K**. Human hand impedance characteristics during maintained posture.
683 *Biol Cybern* 72: 475-485, 1995.
684 **Van Bolhuis B, and Gielen C**. A comparison of models explaining muscle activation patterns for isometric
685 contractions. *Biol Cybern* 81: 249-261, 1999.
686 **Verdaasdonk BW, Koopman HFJM, van Gils SA, and van der Helm FCT**. Bifurcation and stability
687 analysis in musculoskeletal systems: a study in human stance. *Biol Cybern* 91: 48-62, 2004.

688 **Wagner H, and Blickhan R**. Stabilizing function of skeletal muscles: an analytical investigation. *J Theor Biol*

689 199: 163-179, 1999.

690 **Zajac FE**. Muscle and tendon: properties, models, scaling, and application to biomechanics and motor control.

691 *Crit Rev Biomed Eng* 17: 359-411, 1989.

692

693

Acknowledgements

The authors would like to thank Dr. KRS Holzbaur for assistance with the musculoskeletal model, including sharing of the most recent experimental parameters.

Grants

This work was supported by NIH R01 NS053813 and the Searle Funds of the Chicago Community Trust.

Disclosures

No conflicts of interest (financial or otherwise) are declared by the authors.

Figure legends

Figure 1 Single joint elbow stiffness predictions from short-range stiffness (SRS) model, compared with two experimental measurements (Cannon and Zahalak 1982; Perreault et al. 2001). The kinematic parameters of the model were matched to those of subject 4 in Perreault (2001). Negative torque is extension; positive torque is flexion. The experimental data shown are averages across all the subjects in each study. The elbow stiffness reported in Perreault's study was transformed from measured endpoint stiffness of the human arm. Shaded areas show the 95% confidence intervals of the experimental data. The 95% confidence interval of Cannon's study (1982) was computed based on the data of 10 subjects.

Figure 2 Endpoint stiffness predictions from short-range stiffness (SRS) model at three arm positions (the medial, the central and the lateral position), compared with one previous experimental study (Perreault et al. 2001). The kinematic parameters of the model were matched to those of subject 4 in the experimental study. Each ellipse is centered at a location proportional to the endpoint force direction and magnitude the subject was exerting.

Figure 3 **A, B** Elbow joint stiffness and endpoint stiffness model estimates based on the slope of the force-length relationship. The experimental data show Figure 1 are repeated here for comparison (Cannon and Zahalak 1982; Perreault et al. 2001). **A** shows the elbow joint stiffness estimation. **B** shows the endpoint stiffness estimation at the central arm position.

Figure 4 **A, B** The comparison between the average total muscle volume of male subjects and the subject-specific total muscle volume of subject F1, M1 and M5. **A** indicates the variations of stiffness orientation in absolute unit (degrees). **B** indicates the variations of stiffness shape and area normalized by their nominal values.

Table legends

Table 1 Comparison of experimental and model-based estimates of endpoint stiffness.

Table 2 Expected variation of model outputs over the range of plausible model parameters.

738 ## Tables

739 Table 1: Comparison of experimental and model-based estimates of endpoint stiffness.

740

	Arm Position	VAF (%)		
		Orientation	Shape	Area
Short-range stiffness model	Medial	97±2	88±6	80±19
	Central	99±1	93±1	85±4
	Lateral	98±1	91±3	81±11
F-L relationship	Central	84±7	57±22	13±2
Coupled F-L relationship	Central	82±10	55±20	20±6

741 Values in the table are means ± SD.

742

743

744 Table 2: Expected variation of model outputs over the range of plausible model parameters.

	Orientation (deg)	Shape (%)	Area (%)
Moment arm	6.0	22	23
Tendon stiffness	0.6	2	3
Joint angle	6.3	13	11
Volume fraction	3.4	14	14

745

746

747

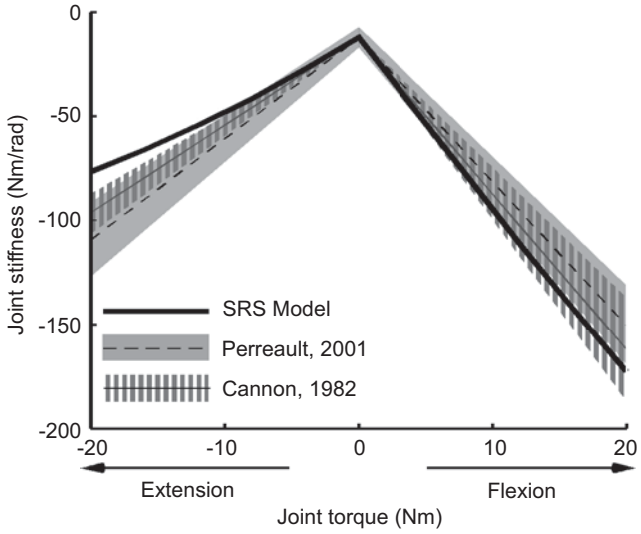
0
-50
-100
-150
-200
Joint stiffness (Nm/rad)
SRS Model
Perreault, 2001
Cannon, 1982
-20
-10
0
10
20
Extension
Flexion
Joint torque (Nm)

Fig 1

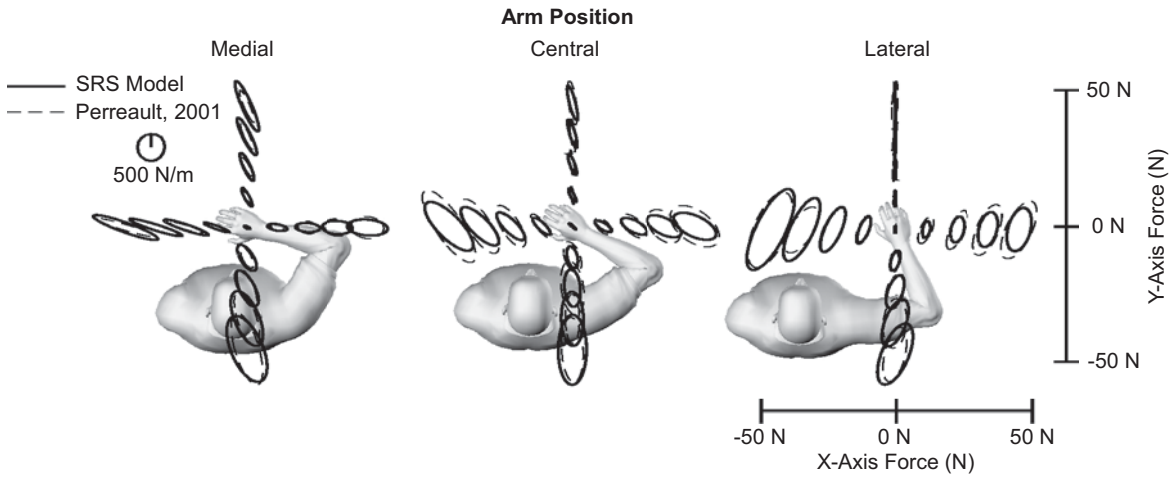
Arm Position
Medial
Central
Lateral
SRS Model
Perreault, 2001
500 N/m
50 N
0 N
-50 N
Y-Axis Force (N)
-50 N
0 N
50 N
X-Axis Force (N)

Fig 2

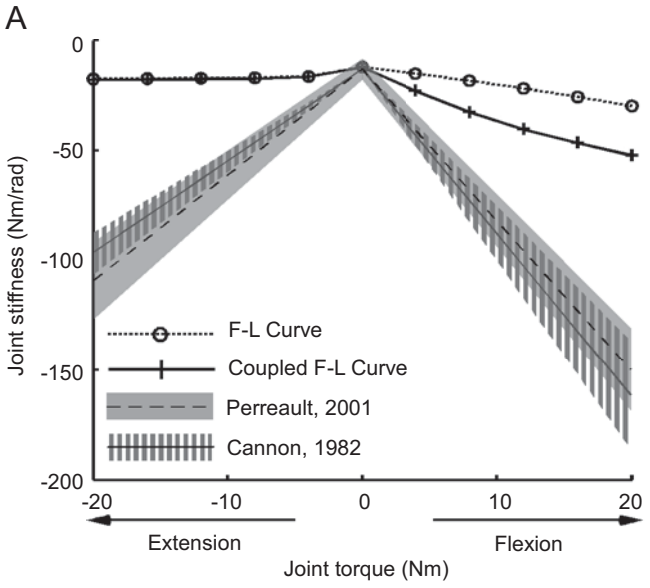
A
0
-50
-100
-150
-200
Joint stiffness (Nm/rad)
F-L Curve
Coupled F-L Curve
Perreault, 2001
Cannon, 1982
-20
-10
0
10
20
Extension
Flexion
Joint torque (Nm)

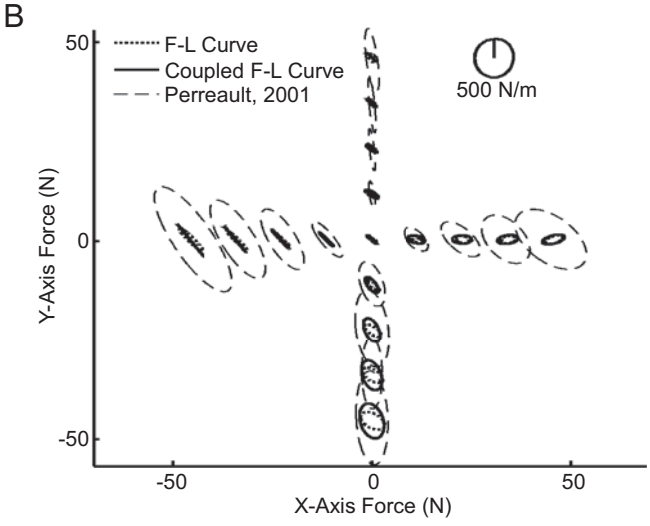
B
50
0
-50
F-L Curve
Coupled F-L Curve
Perreault, 2001
500 N/m
Y-Axis Force (N)
-50
0
50
X-Axis Force (N)

Fig 3

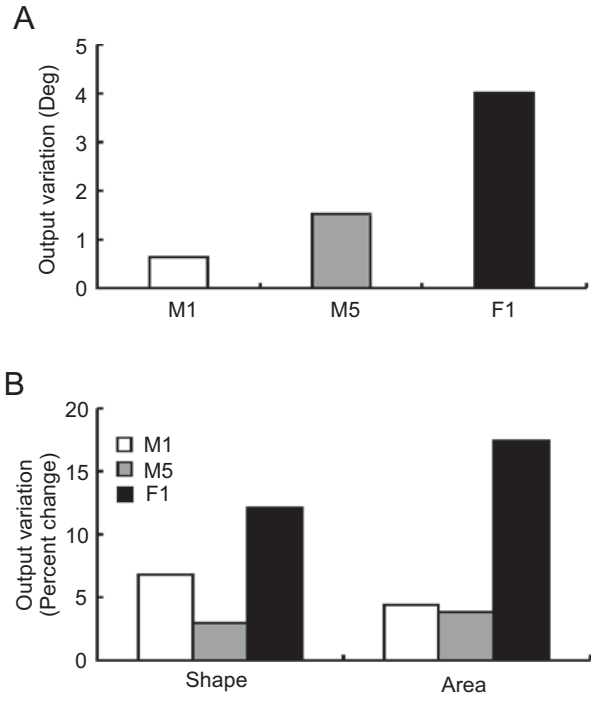
A
Output variation (Deg)
5
4
3
2
1
0
M1
M5
F1
B
Output variation
(Percent change)
20
15
10
5
0
M1
M5
F1
Shape
Area

Fig 4